Article:
Collier, G., Hughes, P., Horn, F. et al. (5 more authors) (2019) Single breath-held acquisition of co-registered 3D 129Xe lung ventilation and anatomical proton images of the human lung with compressed sensing. Magnetic Resonance in Medicine. ISSN 0740-3194

https://doi.org/10.1002/mrm.27713

Single breath-held acquisition of co-registered 3D ^{129}Xe lung ventilation and anatomical proton images of the human lung with compressed sensing

Guilhem J. Collier[1*], Paul J.C. Hughes[1], Felix C. Horn[1], Ho-Fung Chan[1], Bilal Tahir[1,2], Graham Norquay[1], Neil J. Stewart[1], Jim M. Wild[1]

[1]POLARIS, Academic Unit of Radiology, Department of IICD, University of Sheffield, Sheffield, UK; [2]Academic Unit of Clinical Oncology, University of Sheffield, Sheffield, UK

Word count: (1830 words, 3 figures, 2 tables)

Running title: Rapid acquisition of ^{129}Xe and ^{1}H lung MR images with CS

Key Words: hyperpolarized gases, lungs, compressed sensing

[*]Correspondence to: Dr Guilhem J Collier, Academic Unit of Radiology, Department of Infection Immunity and Cardiovascular Disease, University of Sheffield; Floor C, Royal Hallamshire Hospital, Glossop Road, S10 2JF, Sheffield, UK. E-mail: g.j.collier@sheffield.ac.uk

ABSTRACT: (249/250 words max)

Purpose: To develop and assess a method for acquiring co-registered proton anatomical and hyperpolarized ^{129}Xe ventilation MR images of the lungs with compressed sensing (CS) in a single breath-hold.

Methods: Retrospective CS simulations were performed on fully sampled ventilation images acquired from one healthy smoker to optimize reconstruction parameters. Prospective same-breath anatomical and ventilation images were also acquired in five ex-smokers with an acceleration factor of 3 for hyperpolarized ^{129}Xe images, and were compared to fully sampled images acquired during the same session. The following metrics were used to assess data fidelity: mean absolute error (MAE), root mean square error (RMSE) and linear regression of the signal intensity between fully sampled and under-sampled images. The effect of CS reconstruction on two quantitative imaging metrics routinely reported (percentage ventilated volume %VV and heterogeneity score) was also investigated.

Results: Retrospective simulations showed good agreement between fully sampled and CS-reconstructed (acceleration factor of 3) images with MAE (RMSE) of 3.9% (4.5%). The prospective same-breath images showed a good match in ventilation distribution with an average R-squared of 0.76 from signal intensity linear regression and a negligible systematic bias of +0.1% in %VV calculation. A bias of -1.8% in the heterogeneity score was obtained.

Conclusion: With CS, high quality 3D images of hyperpolarized ^{129}Xe ventilation (resolution 4.2x4.2x7.5 mm^3) can be acquired with co-registered ^{1}H anatomical MRI in a 15 s breath-hold. The accelerated acquisition time dispenses with the need for registration between separate breath-hold ^{129}Xe and ^{1}H MRI enabling more accurate %VV calculation.

Key Words: hyperpolarized ^{129}Xe gas, lung MRI, compressed sensing

INTRODUCTION

Lung ventilation MRI with hyperpolarized (HP) noble gases (^{3}He and ^{129}Xe) provides high spatial resolution images of inhaled gas distribution within the lungs. The technique has been shown to be sensitive to different obstructive lung diseases, e.g. chronic obstructive pulmonary disease (1-3), cystic fibrosis (4,5) and asthma (6-8). The acquisition of ^{1}H MR images of the lung is usually performed in the same MRI session in order to observe lung anatomy and structure, but also to delineate the lung cavity for the calculation of the commonly reported percentage ventilated volume (%VV), which is the percentage of the thoracic cavity volume containing HP gas. Both structural and ventilation images are usually obtained in two separate breath-holds and therefore a registration step is required to align the two set of images (3). We have previously demonstrated that same-breath acquisition of both ^{1}H structural and HP gas ventilation MRI (9) provides a more robust method to calculate %VV (10). This approach has been applied to HP ^{3}He ventilation images with compressed sensing (CS) to further shorten the image acquisition time (11), which is important for patients with lung pathologies that make sustained breath-hold challenging. With the limited supply and rising cost of ^{3}He gas, ^{129}Xe provides a cost-effective alternative to ^{3}He (6). But due to its lower gyromagnetic ratio, lower bandwidths are required to obtain reasonable SNR, which increases the acquisition time. As a result, same-breath whole lung coverage acquisition of HP ^{129}Xe ventilation and ^{1}H anatomical images has been challenging and only recently performed using non-Cartesian sampling strategies (12). The purpose of this work is to apply the CS technique (13) to accelerate the acquisition of 3D ^{129}Xe ventilation images and enable same-breath acquisition of co-registered anatomical ^{1}H images. Additionally, the effect of CS reconstruction on two quantitative imaging metrics routinely reported (%VV and heterogeneity score H_{score}) is also investigated.

METHODS

A fully sampled (FS) 3D HP ^{129}Xe ventilation dataset was acquired on a GE HDx 1.5T MR scanner using 1 L of ^{129}Xe at ~13% polarization from one healthy smoker (male, 31 years, FEV_1 z-score>-1.64) in order to perform retrospective CS simulations and optimize the reconstruction parameters. A quadrature flexible transmit-receive ^{129}Xe radiofrequency coil (CMRS, Brookfield, WI) was used and imaging parameters were as follows: 3D balanced steady-state free precession (bSSFP)

pulse sequence (14), 96x78x32 matrix, FOV = 40x32.5x24 cm^3, TE/TR = 3.6/7.6 ms, bandwidth = ±8.06 kHz, scan time of 19 s. An anatomical ^1H image was acquired in a separate breath with a fast spoiled gradient recalled sequence (SPGR) with the same resolution, FOV = 40x40x24 cm^3, TE/TR = 0.6/1.9 ms, bandwidth = ±83.3 kHz, partial-Fourier encoding in the frequency direction and acquisition time of 6 s. The CS simulations were performed in MATLAB (MathWorks, Natick, MA) as described previously (15-17) by empirically testing different undersampling patterns for acceleration factors (AF) of 2, 3, 4 and 5 with different sets of weights that balance data fidelity, image total variation and image sparsity terms in the iterative reconstruction algorithm adapted from Lustig et al (13). The CS reconstruction fidelity was evaluated with different image metrics including mean absolute error (MAE), root mean square error (RMSE) and pixel by pixel linear regression of the signal intensity (images normalized between 0 and 1). The reconstructed and reference FS images at the original acquired size were used and a manually segmented ventilated volume served as the region of interest for the errors and linear regression calculation. The heterogeneity score H_{score} (18) was also evaluated. H_{score} is an imaging metric of the ventilation heterogeneity and was calculated as follows: for each pixel of the ventilated volume, a local coefficient of variation of the signal intensity in the surrounding pixels is computed $H_{i,j,k}$. H_{score} is then defined as the mean value of the distribution of $H_{i,j,k}$. Finally, %VV was also calculated for each AF and for the fully sampled DICOM images using a semi-automated segmentation software (19).

After CS optimization, additional separate breath FS and same-breath CS-accelerated prospective images of both ^1H and HP ^{129}Xe were acquired from five volunteers, all ex-smokers with a smoking history of at least 10 pack years. An AF of 3 (scan time of 6 s) was used for the prospective CS-accelerated ^{129}Xe ventilated images. The gas mixture consisted of 500 mL of HP ^{129}Xe (with recently optimized polarization of ~ 30 % (20)) and 500 mL of N_2 mixed into a 1 L Tedlar bag before being delivered to the volunteers in the MRI scanner for inhalation and imaging. All in vivo MRI experiments were performed under the approval of the UK national research ethics committee and the local NHS research office. %VV and H_{score} from FS and CS datasets were calculated and compared. Bland-Altman analyses were performed to compare FS and CS global H_{score} and slice by slice %VV for all subjects. SNR was calculated for the FS DICOM images selecting a region of interest with fairly homogeneous signal in a middle slice for both lungs. The noise was estimated in a region outside the lung and corrected for Rician distribution according to (21). Additionally,

CS and FS ^{129}Xe ventilation images were registered to each other to evaluate pixel-by-pixel correlation of signal intensity in the ventilated volume.

RESULTS

CS simulations

A good preservation of the ventilation distribution was obtained in retrospectively undersampled and CS-reconstructed images. A summary of estimated errors and quantitative imaging metrics is presented in Table 1. As expected, increasing the AF from 2 to 5 reduced commonalities with the FS reference image, with MAE and RSME increasing from 3.3 to 4.9 %, and 3.8 to 5.9 %, respectively. %VV remained consistent with the FS image value of 94.8 % with differences lying between 0.6 % (AF=2) and 1.5 % (AF=5). A representative coronal slice of a ^{129}Xe ventilation image for each AF is shown in Figure 1 with the corresponding difference map and pixel by pixel comparison of signal intensity. Linear regression gave the lowest R^2 value of 0.86 for AF=5 and highest R^2 value of 0.95 for AF=2. Image features such as vessels (appearing black on ventilation images) and lung edges were well preserved at low AF but became blurred at higher AF (4 and 5) due to the increased low-pass filtering effect of the CS reconstruction and an increasing loss in high spatial frequencies of the k-space data. High AF also resulted in more homogeneous signal distributions and reduction of H_{score} (Figure 2 and Table 1).

Prospective acquisitions

The sampling pattern used for the prospective acquisition (AF=3) in the 5 volunteers is shown in Figure 2.a. The required total breath-hold time was reduced to 15 s (6 s for anatomical ^{1}H, 6 s for HP ^{129}Xe ventilation plus an additional 3 s delay for the scanner hardware to switch between the two transmit-receive frequencies). Figure 3 shows an example of the improved alignment between ^{129}Xe (red) and ^{1}H images (grayscale) due to the same breath acquisition that is facilitated by CS. Remaining misalignments of much smaller intensity between ^{1}H and ^{129}Xe scans were observed in 2 of the 5 subjects (see example of subject slightly relaxing diaphragm in the period between the back-to-back ^{129}Xe and ^{1}H acquisitions in Figure 3.d). However, these misalignments were of the order of the partial-voluming effect that is present in the anterior and posterior slices and could be improved with better breathing maneuver coaching. A comparison between FS and CS imaging

metrics derived for each subject is presented in Table 2. A mean (range) R^2 value of 0.76 (0.42, 0.90) was obtained for the signal intensity linear regression after registration of the ventilated volumes. The lowest value of 0.42 obtained for subject 3 can be explained by a higher noise level (see SNR in Table 2) and an observed difference in lung inflation level between experiments that could be attributed to a sub optimal breathing maneuver performed by the subject. A mean absolute difference of 1.3 % in global %VV was found between prospective FS and CS data sets. When comparing %VV on a slice by slice basis for all subjects, a Bland-Altman analysis gave a negligible bias of +0.1 % with a confidence interval of -6.7 - 6.8 %. However, a consistently lower H_{score} value (Figure 3 and Table 2) was obtained from the CS reconstructed images as previously observed during the CS simulations. A Bland-Altman analysis of H_{score} of the 5 subjects was performed showing a bias of ~ -1.8 % (-0.9 - 4.4 %).

DISCUSSION

We have demonstrated the feasibility of acquiring 3D HP ^{129}Xe lung ventilation images and anatomical ^{1}H images in the same breath using compressed sensing. Results showed minimal estimated errors in the ^{129}Xe ventilation distribution during CS simulations and a good qualitative and quantitative agreement was found between FS and prospective CS datasets for an AF of 3. While improving the reproducibility and the calculation of %VV through the benefits of obtaining ^{1}H and ^{129}Xe images inherently co-registered in the same breath-hold (10), CS also has a negligible influence on the derived %VV values. The mean absolute difference of 1.3 % in global %VV found between prospective FS and CS data sets is below the previously calculated mean inter-observer error in %VV calculation (2.3%) when analyzing FS images with the same software (19). It is also within the same-day reproducibility confidence interval of %VV measurement (±1.52 %) previously reported in Ebner et al (22). Our results are in line with Qing et al. (11) who previously reported that CS was a good candidate to accelerate the acquisition of ^{3}He ventilation and ^{1}H images in the same breath without compromising image fidelity. The assessment of the heterogeneity score H_{score} of the ventilation distribution however suggests that the resulting images tend to have less high spatial frequency detail than fully sampled images. This systematic difference was to be expected and has limited implications due to the fact that H_{score} is already inherently dependent on MRI sequence parameters, such as image resolution or kernel matrix size for local $H_{i,j,k}$ calculation. H_{score} has recently been shown to be an alternative and meaningful

complementary marker to %VV for the description of the ventilation distribution in different population of patients with pulmonary diseases (23) and using CS for the data acquisition should not affect clinical results as long as the same sequence parameters are used between the patient groups being compared. The total acquisition time could be further reduced by applying CS to the proton images as well (e.g. as in (11)). An acceleration factor of 2 for ^{1}H imaging for example (instead of current AF of 1.26 due to partial Fourier encoding) would decrease the total scan time from 15 to 13 s.

With the methods presented here we demonstrate the feasibility of acquiring high resolution ventilation images with 500 mL of HP ^{129}Xe which further establishes the suitability of ^{129}Xe for clinical imaging and assessment of pulmonary diseases. Further work will focus on the clinical application of the technique in patients with lung pathologies.

ACKNOWLEDGMENTS

This work was supported by NIHR grant NIHR-RP-R3-12-027 and MRC grant MR/M008894/1. GlaxoSmithKline (STU100037614) partly funded the PhD of Paul J.C. Hughes. The views expressed in this publication are those of the author(s) and not necessarily those of the NHS, the National Institute for Health Research or the Department of Health.

REFERENCES

1. Kirby M, Svenningsen S, Owrangi A, Wheatley A, Farag A, Ouriadov A, Santyr GE, Etemad-Rezai R, Coxson HO, McCormack DG, Parraga G. Hyperpolarized 3He and 129Xe MR imaging in healthy volunteers and patients with chronic obstructive pulmonary disease. Radiology 2012;265(2):600-610.
2. Kirby M, Mathew L, Heydarian M, Etemad-Rezai R, McCormack DG, Parraga G. Chronic obstructive pulmonary disease: quantification of bronchodilator effects by using hyperpolarized (3)He MR imaging. Radiology 2011;261(1):283-292.
3. Virgincar RS, Cleveland ZI, Kaushik SS, Freeman MS, Nouls J, Cofer GP, Martinez-Jimenez S, He M, Kraft M, Wolber J, McAdams HP, Driehuys B. Quantitative analysis of hyperpolarized 129Xe ventilation imaging in healthy volunteers and subjects with chronic obstructive pulmonary disease. NMR Biomed 2013;26(4):424-435.
4. Bannier E, Cieslar K, Mosbah K, Aubert F, Duboeuf F, Salhi Z, Gaillard S, Berthezene Y, Cremillieux Y, Reix P. Hyperpolarized (3)He MR for Sensitive Imaging of Ventilation Function and Treatment Efficiency in Young Cystic Fibrosis Patients with Normal Lung Function. Radiology 2010;255(1):225-232.

5. Kanhere N, Couch MJ, Kowalik K, Zanette B, Rayment JH, Manson D, Subbarao P, Ratjen F, Santyr G. Correlation of Lung Clearance Index with Hyperpolarized (129)Xe Magnetic Resonance Imaging in Pediatric Subjects with Cystic Fibrosis. Am J Respir Crit Care Med 2017;196(8):1073-1075.
6. Svenningsen S, Kirby M, Starr D, Leary D, Wheatley A, Maksym GN, McCormack DG, Parraga G. Hyperpolarized (3) He and (129) Xe MRI: differences in asthma before bronchodilation. J Magn Reson Imaging 2013;38(6):1521-1530.
7. Altes TA, Mugler JP, 3rd, Ruppert K, Tustison NJ, Gersbach J, Szentpetery S, Meyer CH, de Lange EE, Teague WG. Clinical correlates of lung ventilation defects in asthmatic children. J Allergy Clin Immunol 2015.
8. He M, Driehuys B, Que LG, Huang Y-CT. Using Hyperpolarized 129Xe MRI to Quantify the Pulmonary Ventilation Distribution. Acad Radiol 2016;23(12):1521-1531.
9. Wild JM, Ajraoui S, Deppe MH, Parnell SR, Marshall H, Parra-Robles J, Ireland RH. Synchronous acquisition of hyperpolarised 3He and 1H MR images of the lungs - maximising mutual anatomical and functional information. NMR Biomed 2011;24(2):130-134.
10. Horn FC, Tahir BA, Stewart NJ, Collier GJ, Norquay G, Leung G, Ireland RH, Parra-Robles J, Marshall H, Wild JM. Lung ventilation volumetry with same-breath acquisition of hyperpolarized gas and proton MRI. NMR Biomed 2014.
11. Qing K, Altes TA, Tustison NJ, Feng X, Chen X, Mata JF, Miller GW, de Lange EE, Tobias WA, Cates GD, Jr., Brookeman JR, Mugler JP, 3rd. Rapid acquisition of helium-3 and proton three-dimensional image sets of the human lung in a single breath-hold using compressed sensing. Magn Reson Med 2015;74(4):1110-1115.
12. Tustison NJ, Avants BB, Lin Z, Feng X, Cullen N, Mata JF, Flors L, Gee JC, Altes TA, Mugler Iii JP, Qing K. Convolutional Neural Networks with Template-Based Data Augmentation for Functional Lung Image Quantification. Acad Radiol 2018.
13. Lustig M, Donoho D, Pauly JM. Sparse MRI: The application of compressed sensing for rapid MR imaging. Magn Reson Med 2007;58(6):1182-1195.
14. Stewart NJ, Norquay G, Griffiths PD, Wild JM. Feasibility of human lung ventilation imaging using highly polarized naturally abundant xenon and optimized three-dimensional steady-state free precession. Magn Reson Med 2015;74(2):346-352.
15. Ajraoui S, Lee KJ, Deppe MH, Parnell SR, Parra-Robles J, Wild JM. Compressed sensing in hyperpolarized 3He lung MRI. Magn Reson Med 2010;63(4):1059-1069.
16. Chan HF, Stewart NJ, Norquay G, Collier GJ, Wild JM. 3D diffusion-weighted (129) Xe MRI for whole lung morphometry. Magn Reson Med 2017.
17. Chan HF, Stewart NJ, Parra-Robles J, Collier GJ, Wild JM. Whole lung morphometry with 3D multiple b-value hyperpolarized gas MRI and compressed sensing. Magn Reson Med 2017;77(5):1916-1925.
18. Tzeng YS, Lutchen K, Albert M. The difference in ventilation heterogeneity between asthmatic and healthy subjects quantified using hyperpolarized 3He MRI. J Appl Physiol (1985) 2009;106(3):813-822.
19. Hughes PJC, Horn FC, Collier GJ, Biancardi A, Marshall H, Wild JM. Spatial fuzzy c-means thresholding for semiautomated calculation of percentage lung ventilated volume from hyperpolarized gas and 1 H MRI. J Magn Reson Imaging 2017.
20. Norquay G, Collier GJ, Rao M, Stewart NJ, Wild JM. 129Xe-Rb Spin-Exchange Optical Pumping with High Photon Efficiency. Physical Review Letters 2018;121(15):153201.
21. Gudbjartsson H, Patz S. The Rician distribution of noisy MRI data. Magn Reson Med 1995;34(6):910-914.
22. Ebner L, He M, Virgincar RS, Heacock T, Kaushik SS, Freemann MS, McAdams HP, Kraft M, Driehuys B. Hyperpolarized 129Xenon Magnetic Resonance Imaging to Quantify Regional Ventilation Differences in Mild to Moderate Asthma: A Prospective Comparison Between

Semiautomated Ventilation Defect Percentage Calculation and Pulmonary Function Tests. Invest Radiol 2017;52(2):120-127.

23. Hughes PJC, Smith L, Horn FC, Biancardi A, Stewart N, Norquay G, Rao M, Aldag I, Taylor C, Marshall H, Collier GJ, Wild JM. Assessment of ventilation heterogeneity using hyperpolarized gas MRI histogram analysis. In Proceedings of the 26th annual meeting of ISMRM, Paris, France, 2018. Abstract 2476.

Tables:

Table 1
Errors of the different reconstructions for the coronal image for acceleration factors (AF) of 2 to 5 (MAE: mean absolute error)

AF	MAE	RMSE	H_{score}	%VV
1	-	-	15.5 %	94.8 %
2	3.3 %	3.8 %	13.6 %	95.4 %
3	3.9 %	4.5 %	12.6 %	95.5 %
4	4.1 %	4.9 %	12.0 %	95.9 %
5	4.9 %	5.9 %	11.6 %	96.3 %

Table 2
Summary of whole lung metrics and SNR for each subject imaged with FS and CS (AF=3) ^{129}Xe ventilation MRI

subject	1	2	3	4	5
%VV (FS)	97.5 %	92.2 %	89.6 %	96.1 %	96.6 %
%VV (CS)	98.3 %	93.5 %	90.6 %	93.5 %	95.6 %
H_{score} (FS)	14.4 %	20.1 %	21.9 %	17.1 %	17.3 %
H_{score} (CS)	13.4 %	18.2 %	18.0 %	16.7 %	15.6 %
r^2	0.81	0.90	0.42	0.86	0.82
SNR (FS)	34.3	28.4	20.3	35.2	42.5

Figure captions:

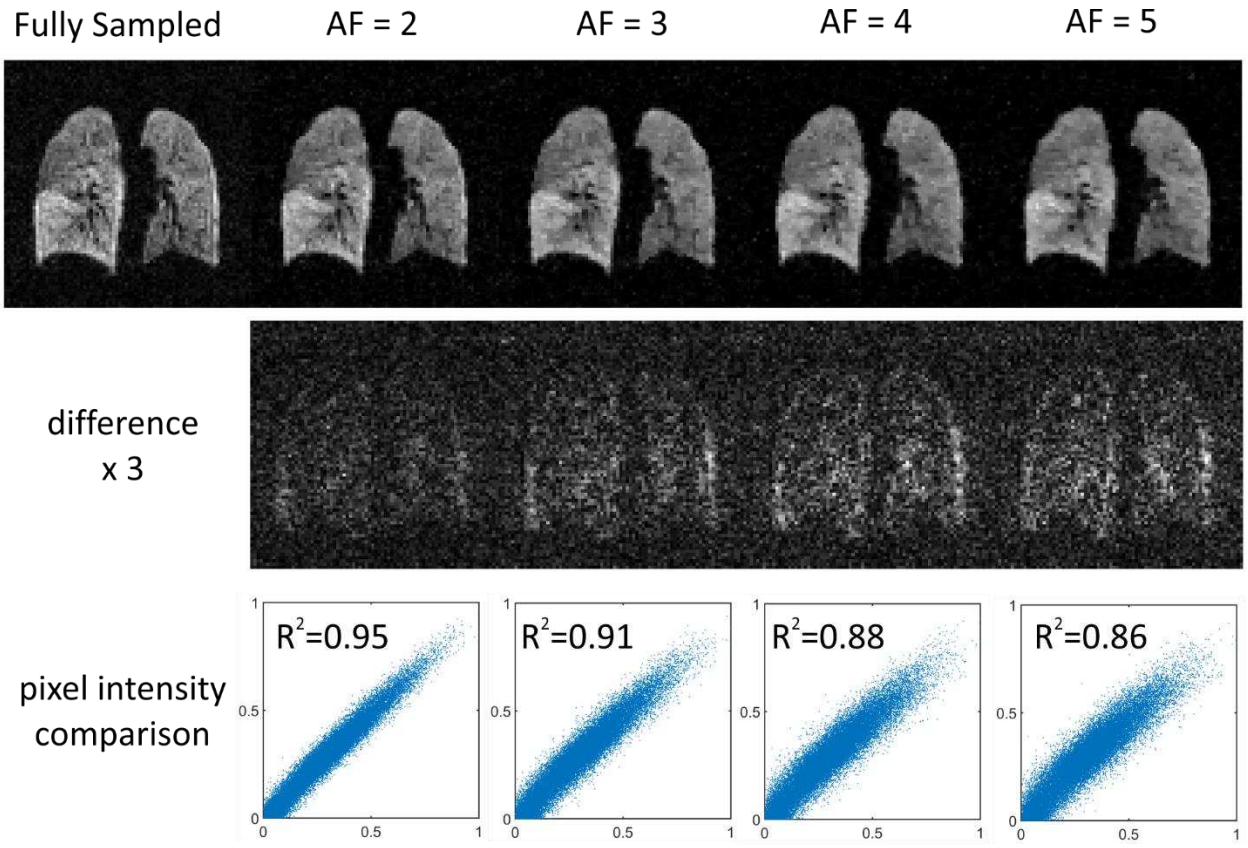

Figure 1: Representative slice of reconstructed dataset after retrospective undersampling (top row), difference images scaled by a factor 3 for reader's clarity (middle row) and pixel by pixel comparison of whole ventilated lung (bottom row) for different acceleration factors.

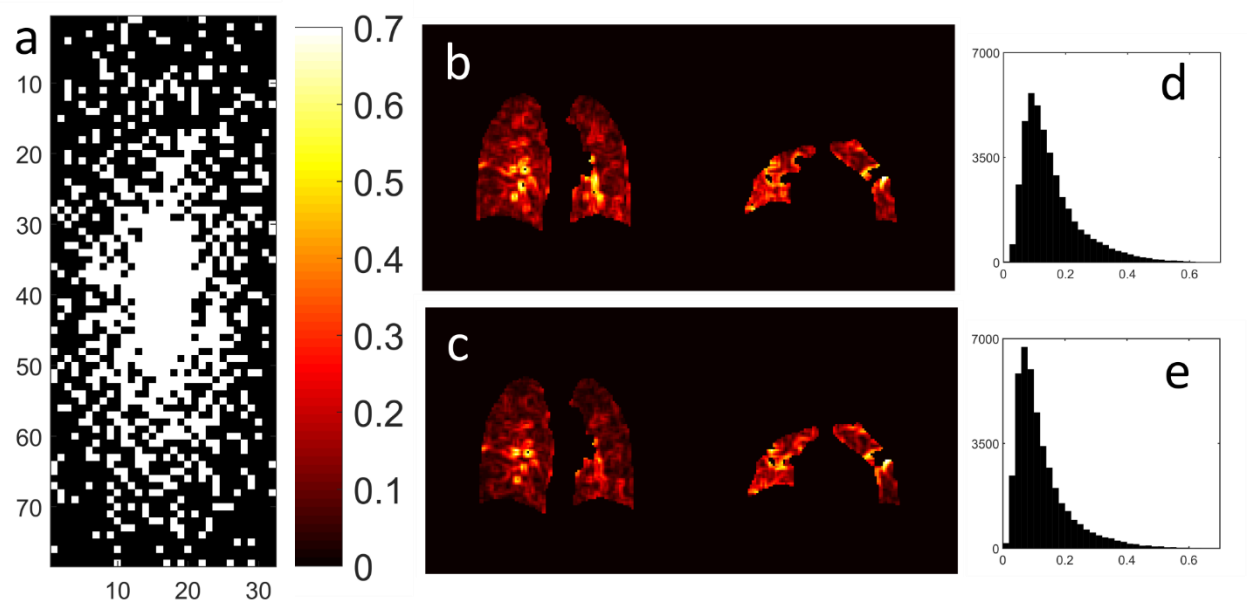

Figure 2: (a) Undersampling pattern for prospective acquisition (AF=3). (b) & (c): Example slices of $H_{i,j,k}$ maps from FS and retrospective CS with AF = 3 respectively. (d) & (e): Corresponding FS and CS $H_{i,j,k}$ histograms.

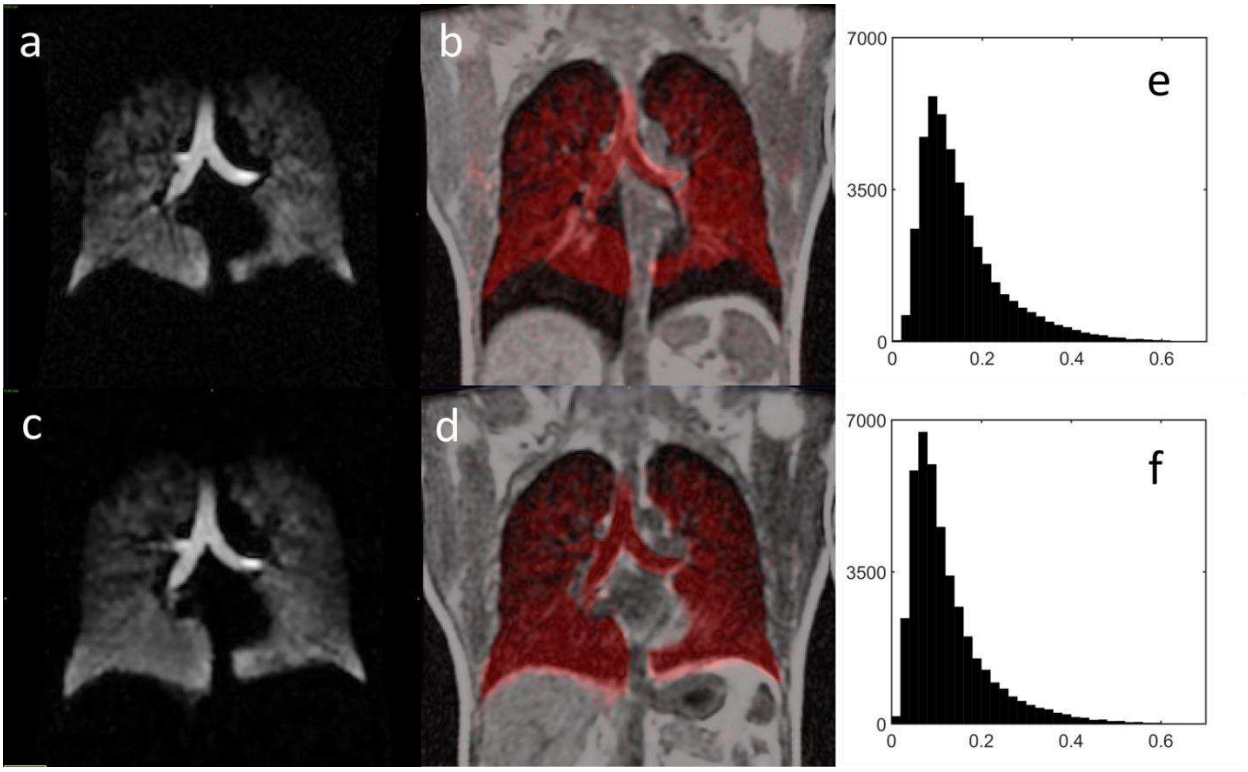

Figure 3: Example of unregistered separate breath FS ^{129}Xe ventilation (a) and ^{1}H images (b). The misalignment is highlighted in (b) by representing the ^{129}Xe image (red) on top of the ^{1}H image (grayscale). (c) & (d): corresponding same breath CS ^{129}Xe and ^{1}H images from the same subject. (e) & (f): ^{129}Xe $H_{i,j,k}$ histograms from FS and CS images.